

Investigating the nature of the Er isotopes with (p, t) reactions

P.E. Garrett^{*†}

Department of Physics, University of Guelph, Guelph, ON N1G2W1, Canada

E-mail: pgarrett@physics.uoguelph.ca

C. Burbadge

Department of Physics, University of Guelph, Guelph, ON N1G2W1, Canada

D. Kisliuk

Department of Physics, University of Guelph, Guelph, ON N1G2W1, Canada

G.C. Ball

TRIUMF, 4004 Wesbrook Mall, Vancouver, BC V6T2A3, Canada

V. Bildstein

Department of Physics, University of Guelph, Guelph, ON N1G2W1, Canada

A. Diaz Varela

Department of Physics, University of Guelph, Guelph, ON N1G2W1, Canada

M.R. Dunlop

Department of Physics, University of Guelph, Guelph, ON N1G2W1, Canada

R. Dunlop

Department of Physics, University of Guelph, Guelph, ON N1G2W1, Canada

T. Faestermann

Physik Department, Technische Universität München, D-85748 Garching, Germany

R. Hertenberger

Fakultät für Physik, Ludwig-Maximilians-Universität München, D-85748 Garching, Germany

D.S. Jamieson

Department of Physics, University of Guelph, Guelph, ON N1G2W1, Canada

K.G. Leach

Department of Physics, Colorado School of Mines, Golden CO, 80401 USA

J. Loranger

Department of Physics, University of Guelph, Guelph, ON N1G2W1, Canada

A.D. MacLean*Department of Physics, University of Guelph, Guelph, ON N1G2W1, Canada***A.J. Radich***Department of Physics, University of Guelph, Guelph, ON N1G2W1, Canada***E.T. Rand***Department of Physics, University of Guelph, Guelph, ON N1G2W1, Canada***B. Rebeiro***Department of Physics, University of the Western Cape, P/B X17, Bellville ZA-7535, South Africa***C.E. Svensson***Department of Physics, University of Guelph, Guelph, ON N1G2W1, Canada***S. Triambak***Department of Physics, University of the Western Cape, P/B X17, Bellville ZA-7535, South Africa***H.-F. Wirth***Fakultät für Physik, Ludwig-Maximilians-Universität München, D-85748 Garching, Germany*

A series of (p,t) reactions have been performed at the Maier-Leibnitz Laboratory using beams of 22 or 24 MeV protons, and the reaction products were analysed with the Q3D spectrograph. The goals of the measurements were to investigate the population of low-lying states in $^{160,162,164,166}\text{Er}$. A number of low-lying 0^+ states have been observed, and their population strengths relative to the ground states extracted. The results confirm the strong population of the 0_2^+ state in ^{164}Er observed previously, and that the 0_2^+ states in $^{160,162}\text{Er}$ are also strongly populated, with strengths in the range of 13% to 20% relative to the ground state population. The strength in ^{160}Er is consistent with that observed in other $N = 92$ isotones, and suggest a common structural feature, possibly related to shape coexistence and the role that the $\frac{11}{2}^- [505]_v$ configuration is playing in the 0_2^+ states in the $N = 90$ isotones.

*The 26th International Nuclear Physics Conference**11-16 September, 2016**Adelaide, Australia*

*Speaker.

†Work supported in part by the Natural Sciences and Engineering Research Council of Canada.

1. Introduction

There continues to be much interest and debate over the nature of excited 0^+ states in nuclei, and even the structure of the 0_2^+ state remains controversial (see, e.g., Refs. [1, 2, 3, 4, 5]). Nuclei at or near $N = 90$ have been studied extensively recently [6, 7, 8, 9, 10, 11, 12, 13, 14, 15, 16] since the suggestion that these nuclei could be at the critical point of a quantum shape phase transition [17, 18, 19, 20, 21]. The rapid transition observed in the structural signatures, such as the energy ratio of the first 4^+ state to that of the first 2^+ state, as well as the $B(E2; 0_1^+ \rightarrow 2_1^+)$ value, as shown in Fig. 1, indicate that a rapid change in shape occurs as a function of neutron number for the rare-earth isotones near $N = 90$. However, whether this is an example of a critical point behaviour of a phase transition, or shape-phase coexistence, is a subtle point (see, e.g., Heyde *et al.* [22]). Critical information in determining the underlying cause of the structural evolution are the nature of the excited states, and especially the excited 0^+ states.

One of best methods of identifying 0^+ states is through the use of two-nucleon-transfer reactions with light-ion beams [23]. In addition to determining the location of excited 0^+ states, they reveal important information on the pairing properties of the states [23]. The ground states of well-deformed nuclei, which are typically in a superfluid state and form a pairing rotational band [23], are populated strongly in (p,t) and (t,p) reactions. The strong populations arise due to the large overlap of the wave functions between the N and $N \pm 2$ system when the pair creation or annihilation operator is applied, and are analogous to the large $B(E2)$ values encountered in a rotational band [23]. For strong population of an excited 0^+ state, this state must also be composed of many terms in the wave function such that a coherent summing of individual amplitudes occurs when the two-particle-transfer operator is applied. An exception to this would be a wave function having a large amplitude by a configuration having low- j values and hence large intrinsic cross sections.

When employed at beam energies typical of tandem accelerators, the (p,t), (t,p), and ($^3\text{He},n$) reactions have very distinctive angular distributions for $L = 0$ transfers from the 0^+ ground states of the even-even targets. However, the shape of the angular distribution is nearly independent of the

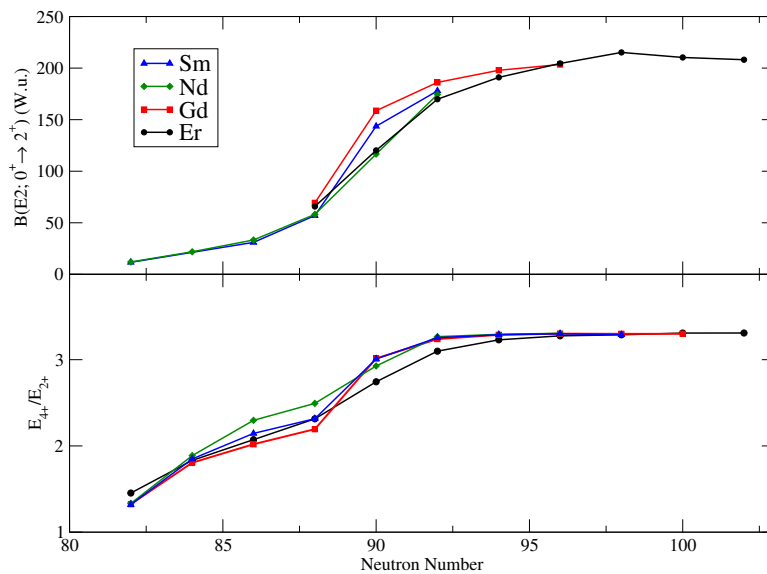


Figure 1: Systematics as a function of neutron number N of the E_{4^+} to E_{2^+} energy ratio (bottom) and the $B(E2; 0_1^+ \rightarrow 2_1^+)$ value in W.u. (top). The rapid change across $N = 90$ is clearly visible. Of note is the strong similarity in the systematics for the isotones of Nd, Sm, Gd, and Er.

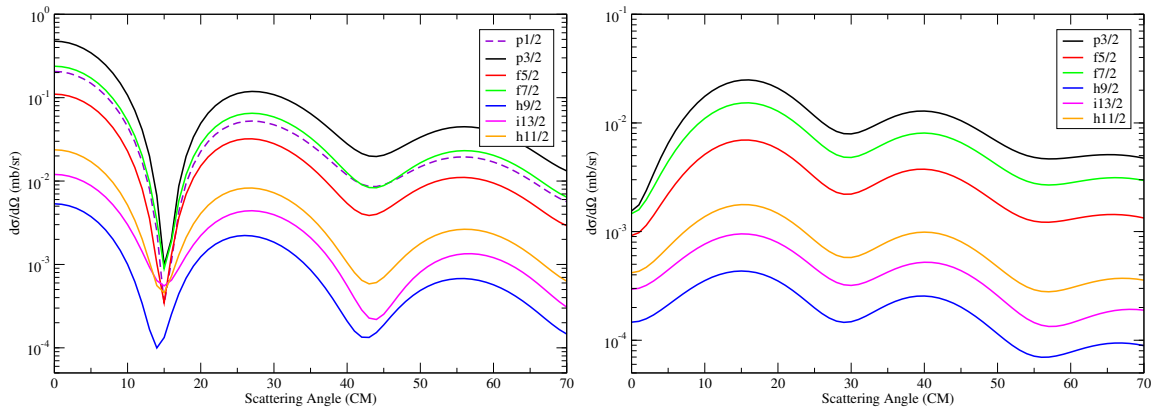


Figure 2: Calculated angular distributions for the $^{162}\text{Er}(p,t)^{160}\text{Er}$ reaction for a 24 MeV proton beam energy. For each curve, the di-neutron form factor is calculated for the single-particle j as labelled. Shown on the left are the angular distributions for $L = 0$ transfers, whereas on the right for $L = 2$ transfers. The angular distributions vary greatly in magnitude, but with little difference in shape.

single-particle j -value of the orbital to/from which they are transferred, as shown in Fig. 2. This is also true for higher L transfers, for example for $L = 2$ also shown in Fig. 2. Thus, in practice unlike single-nucleon transfer where a spectroscopic factor is usually quoted, in two-nucleon-transfer reactions very often the ratios of the excited state cross sections are compared to that of the ground state.

Figure 3 shows the data comparing the relative strength of the population of the low-lying 0^+ and 2^+ states in the $N = 90$ isotones of ^{152}Sm and ^{154}Gd . As can be seen, the 0_2^+ state is strongly populated in both the (t,p) and (p,t) reactions, whereas the 0_3^+ level is strong in the (t,p) , but very weak in the (p,t) reactions. The possible role that the $\frac{1}{2}^- [505]$ neutron orbital could be playing in these excitations has been highlighted by Kulp *et al.* [6, 7] and Sharpey-Schafer *et al.* [12, 13].

In order to extend the systematics in the region, and provide complementary data, we have initiated a systematic study of the Er isotopes using the (p,t) reaction which can be used to reach as far as the $N = 92$ nucleus ^{160}Er . This is made possible due to the possession of unique targets of ^{162}Er and ^{164}Er , which have natural abundances of only 0.14% and 1.6%, respectively, that were

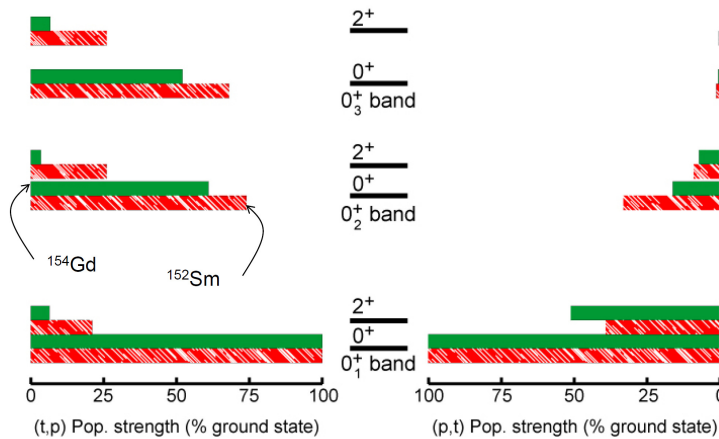


Figure 3: Comparison of the (t,p) (left) and (p,t) (right) strengths relative to the ground state for the $N = 90$ isotones ^{152}Sm (red) and ^{154}Gd (green). Of particular note is the strong population of the 0_2^+ band in both the (t,p) and (p,t) reactions, but very asymmetric population for the 0_3^+ band.

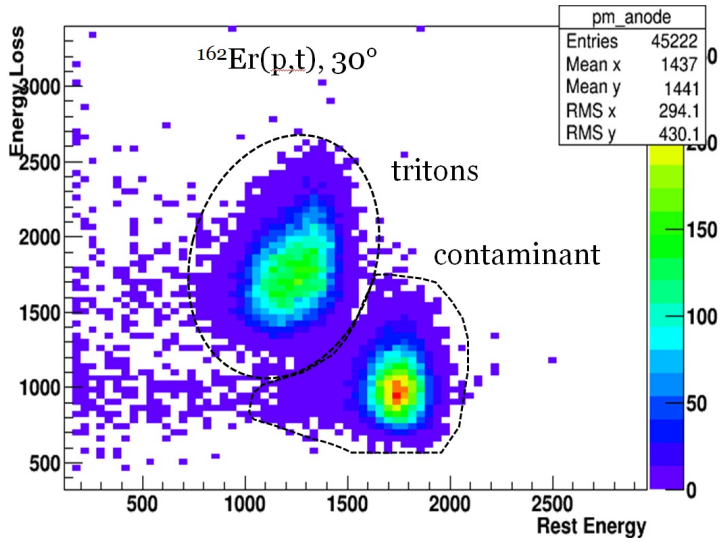


Figure 4: Particle identification plot obtained for the $^{162}\text{Er}(p,t)$ reaction with 24 MeV protons. Plotted is a histogram of the ΔE vs. E where ΔE is derived from an anode layer, and E from a plastic scintillator. For the appropriate settings of the magnets of the Q3D, both tritons and deuterons from reactions on the carbon backing foil (labeled contaminant) of the same magnetic rigidity reach the focal plane detector. The vastly different ΔE vs. E behaviours, however, allows for easy identification on an event-by-event basis.

produced in the 1960's by passing already enriched samples of ^{162}Er and ^{164}Er through a second isotope separator and depositing the material directly onto a carbon foil. The final enrichment of the targets achieved is greater than 99%.

2. Experimental details and results

The experiments were performed at the Maier-Leibnitz Laboratory of the Technische Universität München and Ludwig-Maximilians Universität München using proton beams of 22 or 24 MeV provided by the 15 MV tandem accelerator. The beams of up to $2 \mu\text{A}$ of current impinged on targets of $^{162,164,166,168}\text{Er}$. The products of the reaction were momentum analysed with the Q3D spectrograph, and detected on the focal plane with a detector that provided ΔE - ΔE - E signals for particle identification, as well as the position on the focal plane derived from the position sensitive cathode strip. Figure 4 shows the 2-d particle identification histogram of ΔE vs. E that clearly is able to distinguish the tritons of interest from the deuterons from reactions on the carbon backing foil that have the same magnetic rigidity.

The target thicknesses were determined from measuring the proton elastic scattering cross section, and then normalizing the data to optical model calculations at small scattering angles where the cross section is nearly completely dominated by Rutherford scattering. Angular distributions of the cross sections were constructed from the counts observed via

$$N_c = \frac{d\sigma}{d\Omega} d\Omega N_t N_b (LT) \varepsilon \quad (2.1)$$

where N_c is the number of counts in the peak, $d\Omega$ is the solid angle of the opening of the spectrograph aperture, N_t is the areal density of the target nuclei, N_b the number of beam particles as determined from a Faraday cup placed at 0° downstream of the target, LT is the live time of the detector and data acquisition system combination, and ε is the detector efficiency usually taken to be unity. In practice, since the same spectrograph and detector are used to measure the target thickness, many possible sources of systematic uncertainty are minimized. Shown in Fig. 5 is an example the elastic scattering angular distribution obtained with the ^{162}Er target. In addition to

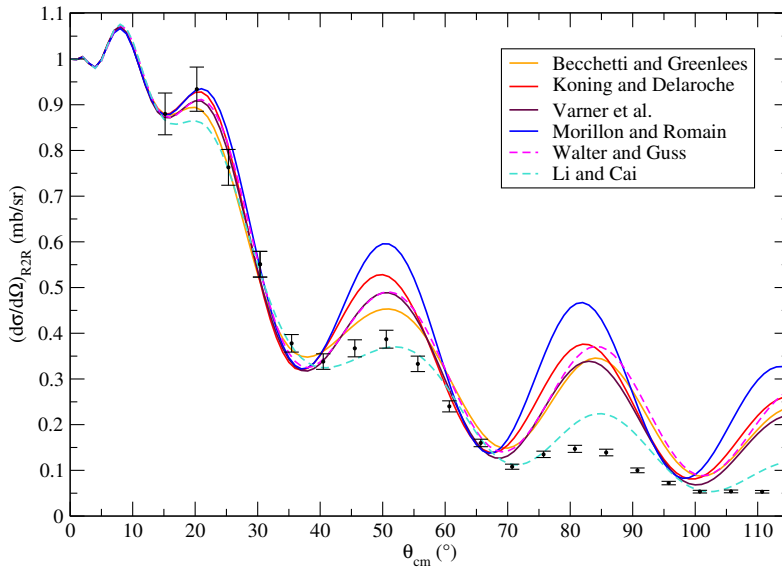


Figure 5: Angular distribution, expressed as a ratio to the Rutherford cross section, of elastically scattered protons observed with $E_p = 24$ MeV from the ^{162}Er target.

the target thickness, these measurements assist in the choice of the most appropriate set of proton optical model parameters to be used in the subsequent calculations.

Shown in Fig. 6 is a portion of the spectrum of tritons observed following the $^{162}\text{Er}(p,t)$ reaction, with some of the more prominent peaks labelled with their excitation energies and I^π values. The ground state band is observed up to spin 6. As can be seen, the 0_2^+ state at 894 keV is very strongly populated, whereas the 0_3^+ level at 1279 keV has approximately an order of

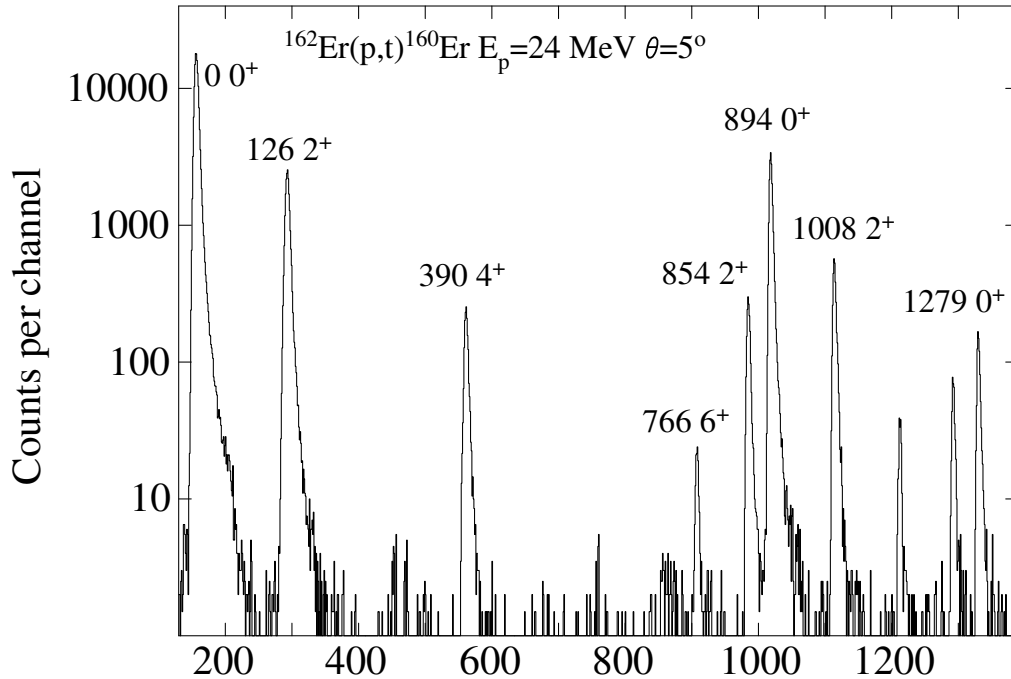


Figure 6: High-momentum portion of the spectrum of tritons observed at 5° following the $^{162}\text{Er}(p,t)^{160}\text{Er}$ reaction with 24 MeV protons.

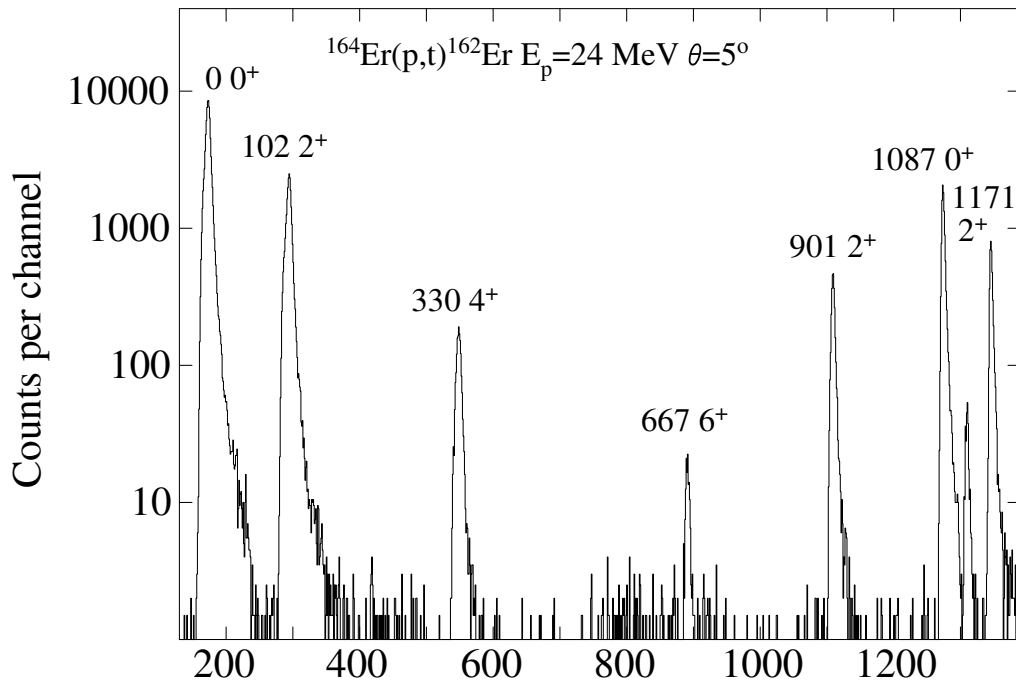


Figure 7: High-momentum portion of the spectrum of tritons observed at 5° following the $^{164}\text{Er}(p,t)^{162}\text{Er}$ reaction with 24 MeV protons.

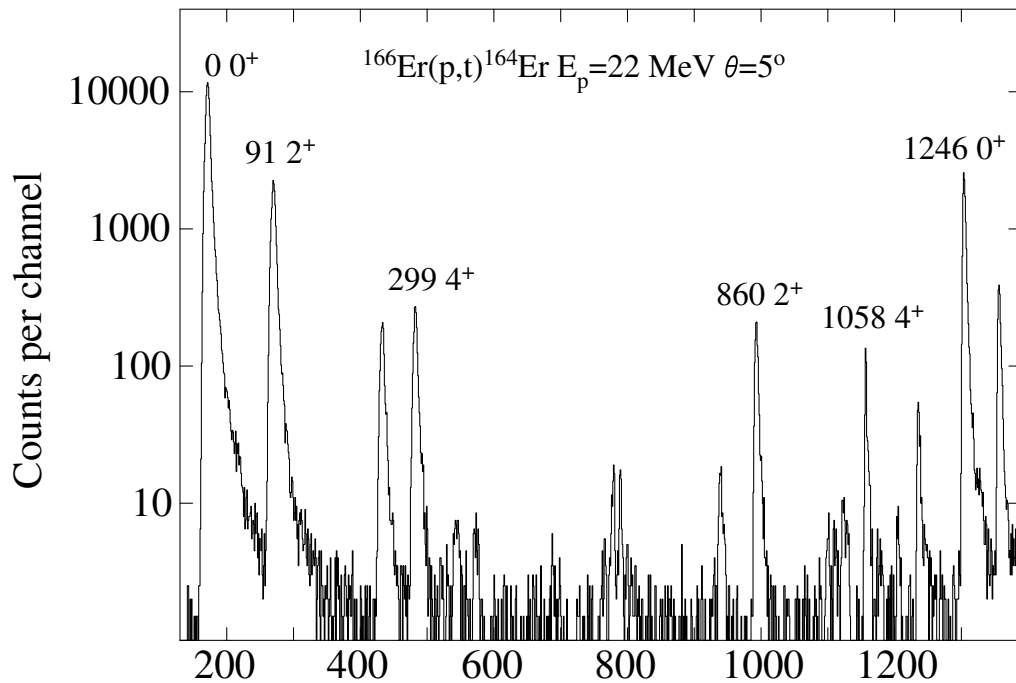


Figure 8: High-momentum portion of the spectrum of tritons observed at 5° following the $^{166}\text{Er}(p,t)^{164}\text{Er}$ reaction with 22 MeV protons.

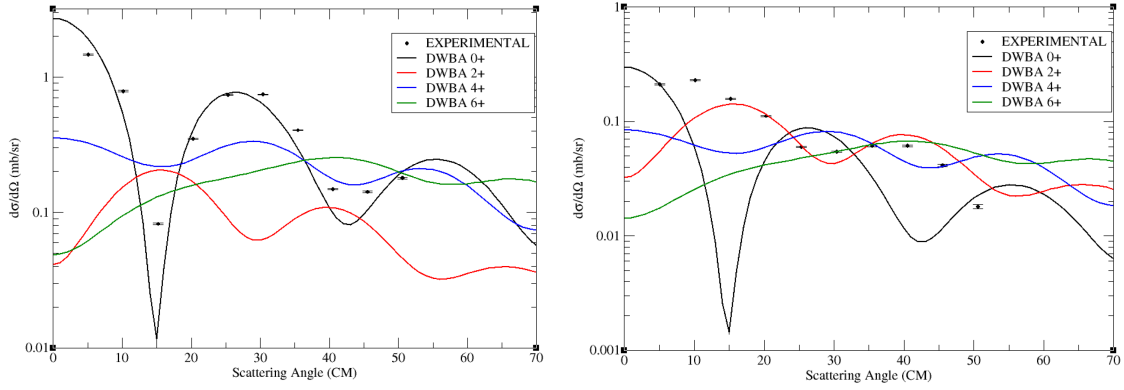


Figure 9: Angular distributions of cross section observed for the $^{162}\text{Er}(p,t)^{160}\text{Er}$ reaction with 24 MeV protons. The left panel shows the cross section for population of the 0^+ ground state, with the right panel that for the 2^+ state.

magnitude smaller cross section. Similarly, in the spectrum shown in Fig. 7, the 0^+ state in ^{162}Er at 1087 keV is also very strongly populated, and in ^{164}Er as well at 1246 keV, shown in Fig. 8.

Some representative angular distributions for the (p,t) reactions are shown in Fig. 9, for the 0^+ ground state and 2^+ first excited state of ^{160}Er . The distinctiveness of the $L=0$ transition can immediately be seen. The higher L transfer curves, especially those to low-lying states, often do not match the predictions of a single step calculation, and to be properly reproduced require coupled-channel calculations. However, the spirit of the present work is not to have a full reproduction of the angular distributions, but to identify and extract excited 0^+ state strength.

3. Discussion

In order to extract the 0^+ population strength relative to the ground state, a correction should be made for Q -value effects. FRESKO calculations were performed for the ground state and excited states and the strength was extracted via

$$S = \frac{\frac{d\sigma}{d\Omega}|_{exp}^{exc}}{\frac{d\sigma}{d\Omega}|_{exp}^{gs}} \cdot \frac{\frac{d\sigma}{d\Omega}|_{DWBA}^{gs}}{\frac{d\sigma}{d\Omega}|_{DWBA}^{exc}} \quad (3.1)$$

where $\frac{d\sigma}{d\Omega}|_{exp}^{exc/gs}$ is the experimental excited state or ground state cross section, and $\frac{d\sigma}{d\Omega}|_{DWBA}^{exc/gs}$ is that from the FRESKO calculations.

In the present work, we concentrate on the strength to the first excited 0^+ state. Shown in Fig. 10 are the strengths, expressed in percent, for the population of the 0_2^+ state relative to the ground state for the $N=92$ isotones. As can be seen, there are consistently strong populations of the 0_2^+ levels for all the isotones where the data are available. This strongly suggests that the 0_2^+ excitations in the $N=92$ isotones are based on a similar structure. Further, examining the systematics as shown in Fig. 11, where strong populations are observed for the 0_2^+ states in $^{160,162,164}\text{Er}$ but become very weak for $^{166,168}\text{Er}$, also suggest that the structure of the 0_2^+ states is similar for $^{160,162,164}\text{Er}$ but changing dramatically for $^{166,168}\text{Er}$. The population observed at $N=92$ for the 0_2^+ level in the (p,t) reaction is very similar to that observed for the (p,t) reaction populating the $N=90$

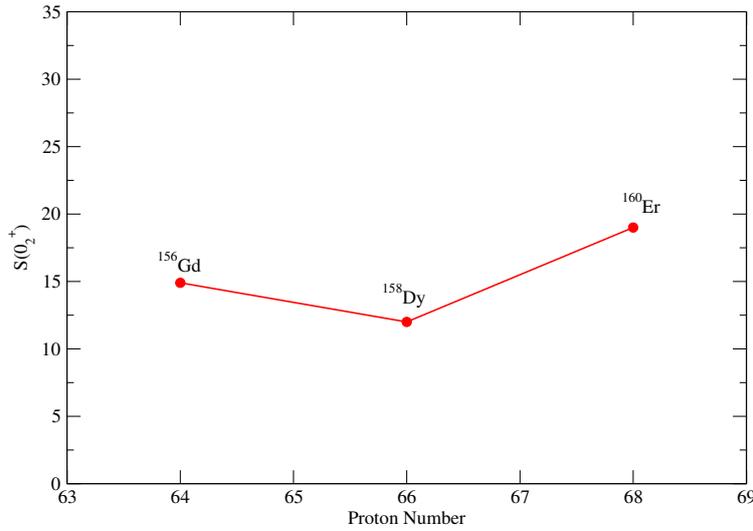


Figure 10: Strength, in percent, for the population of the 0_2^+ state in the $N = 92$ isotones relative to that of the ground state in the (p,t) reactions. The data points are labelled with the residual nucleus.

isotones as shown in Fig. 3. As it has been conjectured [12, 13] that the $\frac{11}{2}^- [505]_v$ configuration is playing a significant role in the 0_2^+ states at $N = 90$, which appear to exhibit shape coexistence, this similarity in population strength at $N = 92$ (and the heavier Er isotopes with $N = 94$ and $N = 96$) may indicate that the same neutron configuration is important for these 0_2^+ states as well.

4. Summary

Excited states of $^{160,162,164,166}\text{Er}$ have been observed with the (p,t) reaction using 22 or 24 MeV proton beams. The reaction products were momentum analysed with a Q3D spectrograph, cross sections determined, and angular distributions produced to locate excited 0^+ states. Strong

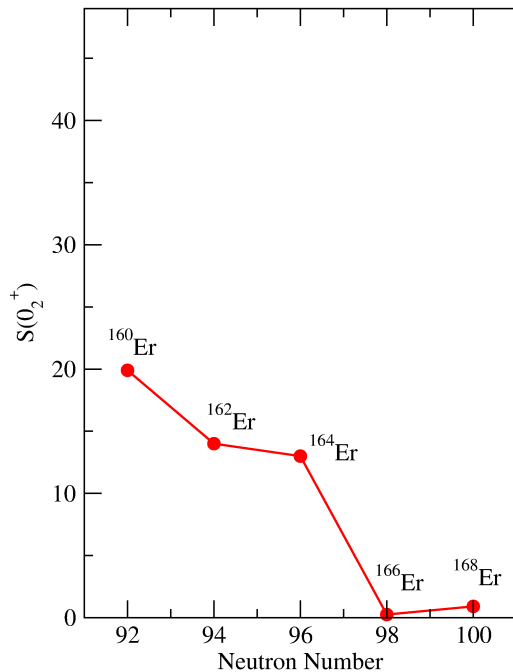


Figure 11: Strength, in percent, for the population of the 0_2^+ state in the Er isotope chain, relative to that of the ground state in the (p,t) reactions. The data points are labelled with the residual nucleus. The similar values for the 0_2^+ states in $^{160,162,164}\text{Er}$ strongly suggest a common structure, whereas that for $^{166,168}\text{Er}$ are likely vastly different.

populations of the 0_2^+ levels in $^{160,162,164}\text{Er}$ were observed, consistent with the strong population in the $N = 92$ isotones of Gd and Dy, and also with nuclei at $N = 90$. The similarity in population strength suggests a similar structure, and it is conjectured that the $\frac{11}{2}^- [505]_v$ configuration may be playing an important role in these states.

References

- [1] P.E. Garrett, J. Phys. G **27**, R1 (2001).
- [2] D. Bonatsos, E.A. McCutchan, and R.F. Casten, Phys. Rev. Lett. **101**, 022501 (2008).
- [3] J.F. Sharpey-Schafer, 50'th International Winter Meeting on Nuclear Physics, Bormio, Italy, Proc. Sci. (Bormio2012) 046 (2012).
- [4] S.R. Lescher *et al.*, Phys. Rev. C **91**, 05431 (2015).
- [5] J.F. Sharpey-Schafer, 54'th International Winter Meeting on Nuclear Physics, Bormio, Italy, Proc. Sci. (Bormio2016) 018 (2016).
- [6] W.D. Kulp *et al.*, Phys. Rev. Lett. **91**, 102501 (2003).
- [7] W.D. Kulp *et al.*, Phys. Rev. C **71**, 041303(R) (2005).
- [8] W.D. Kulp *et al.*, Phys. Rev. C, **76**, 034319 (2007).
- [9] W.D. Kulp *et al.*, Phys. Rev. C **77**, 061301(R) (2008).
- [10] P.E. Garrett *et al.*, Phys. Rev. Lett. **103**, 062501 (2009).
- [11] W.D. Kulp *et al.*, Phys. Rev. C **69**, 064309 (2004).
- [12] J.F. Sharpey-Schafer *et al.*, Eur. Phys. J. A **47**, 5 (2011).
- [13] J.F. Sharpey-Schafer *et al.*, Eur. Phys. J. A **47**, 6 (2011).
- [14] M.A. Caprio *et al.*, Phys. Rev. C **66**, 054310 (2002).
- [15] N. Blasi *et al.*, Phys. Rev. C **90**, 044317 (2014).
- [16] S.N.T. Majola *et al.*, Phys. Rev. C **91**, 034330 (2015).
- [17] F. Iachello *et al.*, Phys. Rev. Lett. **81**, 1191 (1998).
- [18] N.V. Zamfir *et al.*, Phys. Rev. C **60**, 054312 (1999).
- [19] R.F. Casten *et al.*, Phys. Rev. Lett. **82**, 5000 (1999).
- [20] F. Iachello, Phys. Rev. Lett. **87**, 052502 (2001).
- [21] R.F. Casten *et al.*, Phys. Rev. Lett. **87**, 052503 (2001)
- [22] K. Heyde *et al.*, Phys. Rev. C **69**, 054304 (2004).
- [23] R.A. Broglia, O. Hansen, and C. Riedel, Adv. in Nuclear Physics, vol. **6**, eds. M. Baranger and E. Vogt, (Plenum Press, New York, 1973) p.287.